Vol.67: e24230164, 2024
https://doi.org/10.1590/1678-4324-2024230164
ISSN 1678-4324 Online Edition

BABT
Brazilian Archives of Biology and Technology

Article - Engineering, Technology and Techniques

A Robust Day-Ahead UC Model for Hydro-Thermal-Wind Power Systems under Uncertainties

Pricila Cerezolli[1]
https://orcid.org/0000-0002-8020-1210

Rafael Silva Pinto[1]
https://orcid.org/0000-0002-0574-1444

Clodomiro Unsihuay-Vila[1]
https://orcid.org/0000-0002-1639-7765

[1]Universidade Federal do Paraná, Departamento de Engenharia Elétrica, Curitiba, Paraná, Brasil.

Editor-in-Chief: Alexandre Rasi Aoki
Associate Editor: Daniel Navarro Gevers

Received: 19-Feb-2023; Accepted: 20-Oct-2023

*Correspondence: pricilacerezolli@gmail.com; Tel.: +55-49-984318893 (P.C.)

HIGHLIGHTS

- Robust UC model for hydro-thermal-wind power systems under uncertainties.
- Uncertainties on water were modeling considering the spatial and temporal relation.
- Hydro production function was linearized through a piecewise linear approximation.
- Constraints that couple problem in space and time strongly influence the simulation.

Abstract: Energy sources, like hydro and wind power, present uncertain nature, characteristic that affects the electric power systems operation planning. Such factors require using methodologies capable to handle these uncertainties in interconnected hydro-thermal-wind power systems operation. This work proposes a computational model for the day-ahead unit commitment problem for interconnected hydro-thermal-wind power systems, considering the uncertainties related to wind power, water inflow, and energy demand, employing the Robust Optimization (RO). The optimization model consists in a three-level mixed integer linear programming problem, which is resolved using a two-stage decomposition approach, solved using the column-and-constraint generation algorithm. The model is validated using the 30 nodes IEEE and the 33 nodes Brazilian test system. The model proposed proved to have an operating cost proportional to the level of uncertainty and the methodology employed provides a preventive view of what may occur during the hydro-thermal-wind systems operation, allowing the central system operator to take certain actions in order to ensure reliable operating conditions. In addition, the model allowed the identification of important aspects related to computational costs, such as the verification that constraints that couple the problem in time and space significantly impact the simulation times of the problem.

Keywords: Operation planning; Day-ahead UC; Hydro-thermal-wind power systems; Robust optimization (RO); Column-and-constraint generation algorithm (C&CG); Optimization under uncertainty.

INTRODUCTION

The use of alternative sources to electrical generation, together with the growth prospects for the coming years, brings some challenges in terms of electric power systems (EPSs) operation planning. Alternative energy sources, such as wind, are characterized with a very different behavior from conventional sources, as they are intermittent nature, adding a high degree of uncertainty to the EPSs operation [1]. Hydroelectric generation itself, which depends on the volume of water stored in the reservoir, and also on the natural water inflow, presents a certain degree of uncertainty due to the randomness related to the hydrological regime of the rivers, which may vary in the predicted values provided. Likewise, in practice, energy demand is considered a high source of uncertainty due to factors associated to the climate issues that are directly related to forecast errors [2], or even in demand response policies demand [3]. The increase of uncertainty sources in EPSs has made the operation planning more challenging, because these uncertainties must be appropriate considered to obtain models that are closer to the reality and computationally treatable.

In this sense, two methodologies stand out in solving problems under uncertainty: robust optimization (RO) and stochastic programming (SP). The SP assumes that the probability distribution function of uncertain parameters is known, which allows the generation of scenarios to represent the uncertainties. In addition, a large number of scenarios may be necessary to represent the uncertainties, which increases the computational complexity [4]. On the other hand, the RO uses limited sets to represent uncertain parameters, where the previous knowledge of the probability distribution of uncertainty sources is not necessary.

There are several works developed in the operation planning under uncertainties, which employ RO. [5], is one of the first works that uses RO within the EPSs operation, where the objective is to determine the best decisions when the worst-case contingency occurs in an unit commitment (UC) problem. [6] continues this work, with the difference that in this case both contingencies related to lines and generators and also transmission network constraints are considered. Other works developed within RO that also take into account the contingency constraints are [7], [8] and [9].

In regard of RO in UC problems, other relevant works can also be mentioned, such as [10], [11], [12], [13], [14], [15], and [16]. Regarding the consideration of hydro modeling in the RO problem, it is also worth mentioning the work of [17], where the development of a robust two-stage model to solve the UC problem of a hydrothermal system is proposed, where only the uncertainties related to water inflow are taken into account. The construction of the uncertainties sets is made with the use of a vector autoregressive. Regarding the problem of energy economic dispatch and the optimal power flow involving the RO, works like [1], [18], [19] and [20] can be mentioned.

Other works, besides RO, that using different approaches to incorporate the uncertainties to the problem can also be mentioned. In [21], for example, a new approach to solve the thermal-wind-solar power system optimal scheduling problem, including photovoltaic storage is proposed. The uncertainties on wind, solar and load demand are considered. The proposed model handles the sources of uncertainty through the anticipated real time adjustment bids. The model is formulated as a two-stage optimization problem, which consists of a genetic algorithm-based day-ahead optimum scheduling and a two-point estimate based probabilistic real time optimal power flow. [22] proposes an optimal scheduling of wind-thermal power system. The problem formulation also considered the best allocation of spinning reserve and, the uncertainty behavior of wind is handled over the Weibull probability density function. The clustered adaptive teaching learning-based optimization algorithm is used to solve the proposed model. As [22], in [23] a wind-thermal power system is also considered. The uncertainties related to wind are represented over Weibull probability density function. The model consists in a multi-objective optimal power flow where, besides the objective of minimizing the total operation costs, the problem also has other two objectives, transmission losses, and voltage stability enhancement index are selected. The glowworm swarm optimization algorithm is used to solve the problem. The work proposed on [24] is like to [23]. The three objectives are the same, but in [24] the solar photovoltaic units with battery energy storage are also considered. As is done regard the uncertainties on wind, the uncertainty on solar is handled over Weibull probability distribution function. The particle swarm optimization based fuzzy satisfaction maximization technique is used to solve de multi-objective optimal power flow for the wind-thermal-solar system. [25] proposes an optimal power flow on a wind-thermal power system, aiming to minimize the operation costs, and the emissions of nitrogen, carbon and sulfur oxides. The variability in wind is represented over the Weibull probability distribution function, and the opposition based bacterial dynamics algorithm is used to solve the model. [26] also presents a multi-objective optimization problem, aiming to minimize besides the generating costs, the emissions and the reliability. A thermal-wind-solar power system is considered, where the uncertainties on the renewable energy sources (wind and solar), the generator outages and the load forecasted errors are considering over the loss of load probability and the expected unserved energy. In this study the NSGA-II algorithm is used to solve de problem formulation. In

[27] a multi-objective economic dispatch is proposed, where the objectives are to minimize the operation costs and the emission levels. A wind-solar-thermal power system is considered, where the uncertainties on renewable resources are incorporated to the problem over the probability distribution analysis. The thermal problem is formulated considering the nonlinear constraints and the particle swarm optimization algorithm is used to solve the proposed formulation.

Considering the scope of the present work, in the most of these studies that involving RO, only hydrothermal or thermo-wind power systems are considered. Thus, aiming to contribute in this field of study that has a huge relevance, the main objective and contribution of this work is to formulate a RO model to the day-ahead UC problem for a hydro-thermal-wind power systems, considering uncertainties in demand, wind power and water inflow (hydro system). In addition, the energy reserve and transmission network constraints are also modeled.

Therefore, the main contributions to UC RO models presents in this work are: (1) To model the hydro-thermal-wind power system operation planning considering the uncertainties related to wind power, water inflow and demand; (2) To consider the transmission network, using the DC model; (3) To consider the energy reserve; (4) To use a piecewise linear (concave) model to represent the hydroelectric production function; (5) To formulate the complete optimization model using the RO approach in the day-ahead UC problem of the hydro-thermal-wind power system under uncertainties; (6) To implement computationally the proposed mathematical model and analyze it in the 30 nodes IEEE test system (30-IEEE), and in the 33 nodes south Brazilian test system (33-BTS).

It is also noteworthy to the best of authors' knowledge that until then it was not identified in the literature a work that addressed the day-ahead UC problem under uncertainties in demand, water inflow and wind energy, as it is done in this work.

MATERIAL AND METHODS

Problem formulation

Interesting references about RO can be mentioned, such as [28], [29], [30] and [31]. The UC problem is formulated for a hydro-thermal-wind power system under uncertainty using the RO approach. The main objective is to minimize the operating costs of a hydro-thermal-wind power system given the worst realization of uncertainties. A graphical representation of the problem addressed in this study is presented in Figure 1.

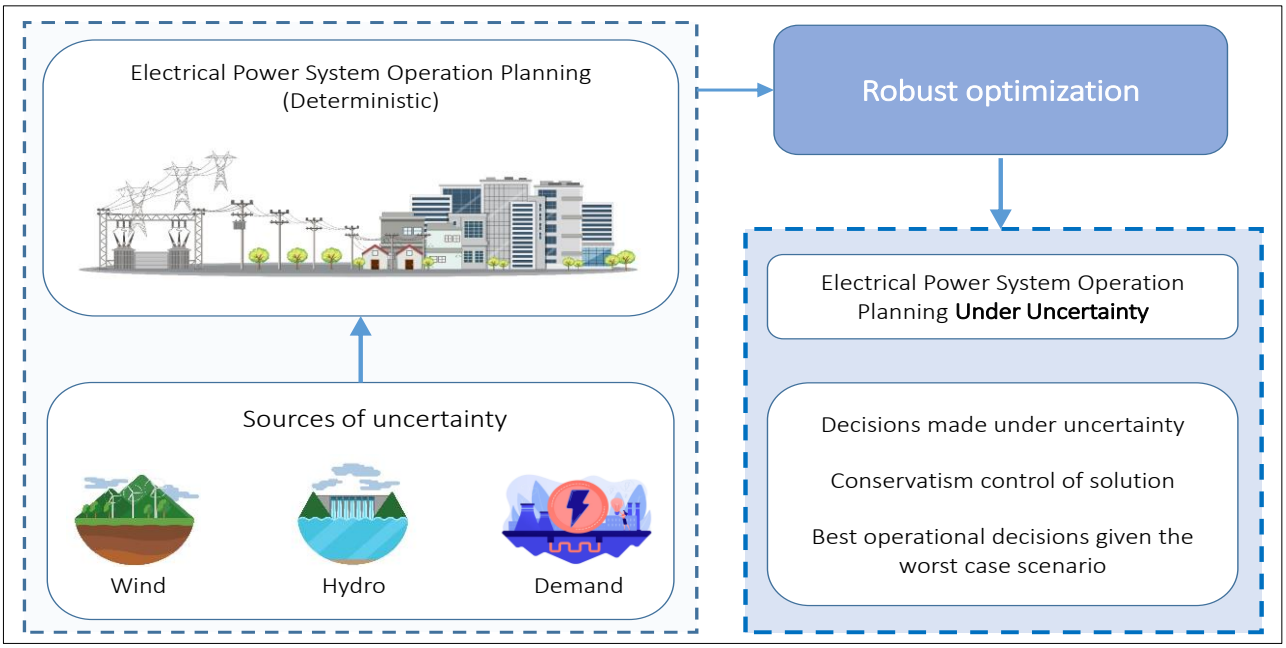

Figure 1. A graphical representation of the problem addressed in this study. The uncertainties related to demand, wind and hydro sources are incorporated to the deterministic electrical power system operation planning through robust optimization. The resulted model allows to obtain the best operational decisions given the worst realization of uncertainties.

The RO model for UC problem addressed in this study, presents decisions made in two stages, and thus formulated as a three level optimization problem. The uncertainties related to wind generation ($\tilde{P}_{w,t}$), the natural water inflow ($\tilde{A}_{r,t}$) and energy demand ($\tilde{P}_{\mathrm{d},t}$) are considered in this work, and their model were formulated based in [11], [15], [17] and [32], where polyhedral geometry is considered. Uncertainties are denoted as $u \in \mathcal{U}$, where u represents each uncertainty variables considered ($u = \{\tilde{P}_{w,t}, \tilde{A}_{r,t}, \tilde{P}_{\mathrm{d},t}\}$), and $\mathcal{U}$ is the polyhedral uncertainty set, which includes the uncertainty set in demand $\mathcal{U}_D$, in wind generation $\mathcal{U}_W$ and water inflow $\mathcal{U}_H$. The main objective of these sets is to determine the value that the uncertain parameters ($\tilde{A}_{r,t}$, $\tilde{P}_{\mathrm{d},t}$ and $\tilde{P}_{w,t}$) should assume.

The uncertainty sets are therefore formulated according to the constraints (1) to (8). Constraint (1) indicates that the set is formed by $\mathcal{U}_H$, $\mathcal{U}_W$ and $\mathcal{U}_D$. Constraints (2) and (3), (4) and (5), and (6) to (8), model each of these sets representing, respectively, the uncertainty in demand, wind and water. The uncertainties constraints in the water inflow are able to represent both the spatial – (6), and the temporal relationship – (7), from the water problem. Constraint (6) limits the total water inflow of the system in each period, while the constraint (7) establishes water inflow limits for each reservoir along the operating horizon. Thus, the limitation of total water inflow through this set of inequalities reflects the spatial dependence between water reservoirs and the temporal dependence of the problem [17].

Uncertainty sets are bounded by the uncertainty level or budget Γ. This, can present values between 0 and 1.The higher the uncertainty level Γ, the greater the deviation that the uncertain parameters can assume – this uncertainty value being limited by (3), (5) and (8).

$$\mathcal{U} = \{\mathcal{U}_D, \mathcal{U}_W, \mathcal{U}_H\} \tag{1}$$

$$\mathcal{U}_D \coloneqq \left\{ \tilde{P}_{\mathrm{d},t} : \frac{\sum_{\mathrm{d}\in\mathcal{D}} \left(\tilde{P}_{\mathrm{d},t} - \hat{P}_{\mathrm{d},t}^{min}\right)}{\sum_{\mathrm{d}\in\mathcal{D}} \left(\hat{P}_{\mathrm{d},t}^{max} - \hat{P}_{\mathrm{d},t}^{min}\right)} \leq \Gamma^D \qquad \forall t \in \mathcal{T}, \right. \tag{2}$$

$$\left. \tilde{P}_{\mathrm{d},t} \in \left[\hat{P}_{\mathrm{d},t}^{min}, \hat{P}_{\mathrm{d},t}^{max}\right] \qquad \forall \mathrm{d} \in \mathcal{D} \right\} \tag{3}$$

$$\mathcal{U}_W \coloneqq \left\{ \tilde{P}_{w,t} : \frac{\sum_{w\in\mathcal{W}} \left(\hat{P}_{w,t}^{max} - \tilde{P}_{w,t}\right)}{\sum_{w\in\mathcal{W}} \left(\hat{P}_{w,t}^{max} - \hat{P}_{w,t}^{min}\right)} \leq \Gamma^W \qquad \forall t \in \mathcal{T}, \right. \tag{4}$$

$$\left. \tilde{P}_{w,t} \in \left[\hat{P}_{w,t}^{min}, \hat{P}_{w,t}^{max}\right] \qquad \forall w \in \mathcal{W} \right\} \tag{5}$$

$$\mathcal{U}_H \coloneqq \left\{ \tilde{A}_{r,t} : \frac{\sum_{r\in\mathcal{R}} \left(\hat{A}_{r,t}^{max} - \tilde{A}_{r,t}\right)}{\sum_{r\in\mathcal{R}} \left(\hat{A}_{r,t}^{max} - \hat{A}_{r,t}^{min}\right)} \leq \Gamma^H \qquad \forall t \in \mathcal{T}, \right. \tag{6}$$

$$\frac{\sum_{t\in\mathcal{T}} \left(\hat{A}_{r,t}^{max} - \tilde{A}_{r,t}\right)}{\sum_{t\in\mathcal{T}} \left(\hat{A}_{r,t}^{max} - \hat{A}_{r,t}^{min}\right)} \leq \Gamma^H \qquad \forall r \in \mathcal{R}, \tag{7}$$

$$\left. \tilde{A}_{r,t} \in \left[\hat{A}_{r,t}^{min}, \hat{A}_{r,t}^{max}\right] \qquad \forall r \in \mathcal{R} \right\} \tag{8}$$

Uncertainty in wind generation, as well as the other sources of uncertainty considered, is modeled considering a possible variation between $\hat{P}_{w,t}^{min}$ and $\hat{P}_{w,t}^{max}$. The value that $\tilde{P}_{w,t}$, in addition to depend on $\hat{P}_{w,t}^{min}$ and $\hat{P}_{w,t}^{max}$, it also depends on the assumed Γ^W. By setting $\Gamma^W = 1$, the maximum possible wind generation deviation can occur, indicating that the $\tilde{P}_{w,t}$ can take any value between $\hat{P}_{w,t}^{min}$ and $\hat{P}_{w,t}^{max}$. Analyzing the worst-case scenario in this situation, $\tilde{P}_{w,t}$ will be equal to $\hat{P}_{w,t}^{min}$. In the opposite case, i.e. $\Gamma^W = 0$, $\tilde{P}_{w,t}$ should not deviate from its predicted values, being equal to $\hat{P}_{w,t}^{max}$, as this is equivalent to the deterministic and therefore more optimistic case, where there is no consideration of uncertainty. An aspect that must be noticed is that in this hypothetical example, it is considered that the system is composed only of a wind generator unit and therefore it presents this behavior. In the case of the existence of more wind power plants, the sum of all units must be considered. For example, if there are two wind units and $\Gamma^W = 1$, the sum of uncertain generation of all wind units may vary between $\hat{P}_{w,t}^{min}$ and $\hat{P}_{w,t}^{max}$.

Regarding the maximum and minimum limits of the uncertain variables – (3), (5) and (8), in this work are defined as a percentage change of the expected historical values, however they can be defined also from the physical and operational limits of the system, or even through more sophisticated forecasting methods. It is noteworthy that forecasting methods for both demand, wind generation and water inflow are outside the scope of this work. In the present study, it is assumed that the predicted values for these parameters are already known. It is also worth to mention that this study considers the worst realization of uncertainties for wind generation, as well as for water inflow and energy demand.

The RO model for UC problem formulated in this study is presented according to the formulation (9) to (21). Through this model, it is possible to observe the hierarchical structure of the RO problem with three levels of optimization, which also reflects the nature of decision made in two stages. Thus, the first level refers to commitment decisions of the generating units, while the second and third levels refers to the best operational decisions, given the worst case realization of the uncertainties, that is, the worst case of dispatch cost [11].

$$\min_{x,v} \sum_{t=1}^{T} \sum_{i \in \mathcal{I}_K} \left(C_{i,t}^{SU} + C_{i,t}^{SD} + C_{i,t}^{NL} x_{i,t} \right) + \max_{u \in \mathcal{U}} \min_{y \in \Omega(x,v,u)} \sum_{t=1}^{T} \sum_{i \in \mathcal{I}_K} C_{i,t}^{P} + \sum_{t=1}^{T} \sum_{r=1}^{\mathcal{R}} \hat{C}_{r,t}^{S} S_{r,t} \tag{9}$$

s.t:

$$C_{i,t}^{SU} \geq \hat{C}_i^{SU} \left(x_{i,t} - x_{i,t-1} \right) \qquad \forall i \in \mathcal{I}_K, \forall t \in \mathcal{T} \tag{10}$$

$$C_{i,t}^{SU} \geq 0 \qquad \forall i \in \mathcal{I}_K, \forall t \in \mathcal{T} \tag{11}$$

$$C_{i,t}^{SD} \geq \hat{C}_i^{SD} \left(x_{i,t-1} - x_{i,t} \right) \qquad \forall i \in \mathcal{I}_K, \forall t \in \mathcal{T} \tag{12}$$

$$C_{i,t}^{SD} \geq 0 \qquad \forall i \in \mathcal{I}_K, \forall t \in \mathcal{T} \tag{13}$$

$$x_{i,t} - x_{i,t-1} = v_{i,t}^{SU} - v_{i,t}^{SD} \qquad \forall i \in \mathcal{I}, \forall t \in T \tag{14}$$

$$t_i^{up} = \max \left\{ 0, \left(\hat{T}_i^{up} - \hat{T}_i^{up(0)} \right) x_i^0 \right\} \qquad \forall i \in \mathcal{I} \tag{15}$$

$$t_i^{dn} = \max \left\{ 0, \left(\hat{T}_i^{dn} - \hat{T}_i^{dn(0)} \right) (1 - x_i^0) \right\} \qquad \forall i \in \mathcal{I} \tag{16}$$

$$x_{i,t} = x_i^0 \qquad \forall i \in \mathcal{I}, \forall t \in \left[1, t_i^{up} + t_i^{dn} \right] \tag{17}$$

$$\sum_{\hat{t}=t-\hat{T}_i^{up}+1}^{t} v_{i,\hat{t}}^{SU} \leq x_{i,t} \qquad \forall i \in \mathcal{I}, \forall t \in [\hat{T}_i^{up}, T] \tag{18}$$

$$\sum_{\hat{t}=t-\hat{T}_i^{dn}+1}^{t} v_{i,\hat{t}}^{SD} \leq 1 - x_{i,t} \qquad \forall i \in \mathcal{I}, \forall t \in [\hat{T}_i^{dn}, T] \tag{19}$$

$$\sum_{i \in \mathcal{I}_K} \hat{P}_i^{max} . x_{i,t} + \sum_{i \in \mathcal{I}_H} \hat{P}_i^{max} . x_{i,t} + \sum_{w \in \mathcal{W}} \tilde{P}_{w,t} \geq \sum_{\mathrm{d} \in \mathcal{D}} \tilde{P}_{\mathrm{d},t} \left(1 + \hat{R}^{\%} \right) \qquad \forall t \in \mathcal{T} \tag{20}$$

$$x_{i,t}, v_{i,t}^{SU}, v_{i,t}^{SD} \in \{0,1\} \qquad \forall i \in \mathcal{I}, \forall t \in \mathcal{T} \tag{21}$$

Expression (9) is the objective function where it aims to minimize the costs related to commitment decision of generating units (first stage of the problem – min level) and, from these decisions, the best dispatch solution, given the worst realization of uncertainties must be identified (second stage – $max\ min$ levels). Inequalities (10) to (13) are the on/off decisions to the thermal units, while (14) to (19) are the logic constraints between the binary variables of the hydro and thermal problem and the minimum up and

downtime of each unit. The constraint (20) guarantees the energy reserve and (21) defines the binary variables of the problem.

The set $\Omega(x, v, u)$ in (9), is presented in (22) to (37). This is the set of primal constraints of the third level problem, which represents the viable solution to the dispatch, i.e., it ensures the achievement of a feasible solution to the operational decisions, given the fixed commitment decisions of the generating units (x, v) obtained in the formulation (9) to (21), and the realization of the uncertainty (u) defined by (1) to (8).

$$\Omega(x, v, u) = \Big\{ y \backslash (x, v):$$

$$\sum_{i \in k_n} p_{i,t} + \sum_{i \in h_n} p_{i,t} - \sum_{l \in \ell_{n,s}} P_{l,t} + \sum_{l \in \ell_{n,s}} P_{l,t} = \sum_{\mathrm{d} \in d_n} \tilde{P}_{\mathrm{d},t} - \sum_{w \in w_n} \tilde{P}_{w,t} \qquad \left(\lambda_{n,t}\right) \forall n \in \mathcal{N}, \forall t \in \mathcal{T} \tag{22}$$

$$P_{l,t} = \hat{P}_b \hat{B}_l \left(\theta_{n(s,l),t} - \theta_{n(e,l),t}\right) \qquad \left(\lambda^P_{l,t}\right) \forall l \in \mathfrak{L}, \forall t \in \mathcal{T} \tag{23}$$

$$-\hat{P}_l^{max} \leq P_{l,t} \leq \hat{P}_l^{max} \qquad \left(\phi_{l,t}^{\hat{P}^{max}}, \phi_{l,t}^{\hat{P}^{min}}\right) \forall l \in \mathfrak{L}, \forall t \in \mathcal{T} \tag{24}$$

$$-\pi \leq \theta_{n,t} \leq \pi \qquad \left(\phi_{n,t}^{\hat{\theta}^{max}}, \phi_{n,t}^{\hat{\theta}^{min}}\right) \forall n \in \mathcal{N}, \forall t \in \mathcal{T} \tag{25}$$

$$\theta_{n,t} = 0 \qquad \left(\lambda_{n,t}^{\theta^{ref}}\right) \; i = ref, \forall t \in \mathcal{T} \tag{26}$$

$$C_{i,t}^P \geq \hat{a}_{i,e} p_{i,t} + \hat{b}_{i,e} \qquad \left(\phi_{i,e,t}^{C^P}\right) \forall i \in \mathcal{I}_K, \forall e \in \mathcal{E}, \forall t \in \mathcal{T} \tag{27}$$

$$\hat{P}_i^{min} x_{i,t} \leq p_{i,t} \leq \hat{P}_i^{max} x_{i,t} \qquad \left(\phi_{i,t}^{\hat{P}^{max}}, \phi_{i,t}^{\hat{P}^{min}}\right) \forall i \in \mathcal{I}_K, \forall t \in \mathcal{T} \tag{28}$$

$$p_{i,t} - p_{i,t-1} \leq \hat{R}_i^{UP} x_{i,t-1} + \hat{S}_i^{SU} v_{i,t}^{SU} \qquad \left(\phi_{i,t}^{\hat{R}^{UP}}\right) \forall i \in \mathcal{I}_K, \forall t \in \mathcal{T} \tag{29}$$

$$p_{i,t-1} - p_{i,t} \leq \hat{R}_i^{DN} x_{i,t} + \hat{S}_i^{SD} v_{i,t}^{SD} \qquad \left(\phi_{i,t}^{\hat{R}^{DN}}\right) \forall i \in \mathcal{I}_K, \forall t \in \mathcal{T} \tag{30}$$

$$p_{i,t} \leq \hat{\alpha}_{i,\rho} q_{i,t} + \hat{\beta}_{i,\rho} x_{i,t} \qquad \left(\phi_{i,\rho,t}^{p}\right) \forall i \in \mathcal{I}_H, \forall \rho \in \mathcal{P}, \forall t \in \mathcal{T} \tag{31}$$

$$V_{r,t} = V_{r,t-1} - \hat{C}\left(Q_{r,t} + S_{r,t} - \tilde{A}_{r,t}\right) + \sum_{m \in \mathcal{M}_r} \hat{C}\left(Q_{m,t} + S_{m,t}\right) \qquad \left(\lambda_{r,t}^V\right) \forall r \in \mathcal{R}, \forall t \in \mathcal{T} \tag{32}$$

$$\hat{V}_r^{min} \leq V_{r,t} \leq \hat{V}_r^{max} \qquad \left(\phi_{r,t}^{\hat{V}^{max}}, \phi_{r,t}^{\hat{V}^{min}}\right) \forall r \in \mathcal{R}, \forall t \, \mathcal{T} \; t = T \tag{33}$$

$$\hat{V}_r^{end} \leq V_{r,t} \leq \hat{V}_r^{max} \qquad \left(\phi_{r,t}^{\hat{V}^{fim}}, \phi_{r,t}^{\hat{V}^{max}}\right) \forall r \in \mathcal{R}, t = T \tag{34}$$

$$0 \leq S_{r,t} \leq \hat{S}_r^{max} \qquad \left(\phi_{r,t}^{\hat{S}^{max}}, \phi_{r,t}^{\hat{S}^{min}}\right) \forall r \in \mathcal{R}, \forall t \in \mathcal{T} \tag{35}$$

$$\hat{Q}_i^{min} x_{i,t} \leq q_{i,t} \leq \hat{Q}_i^{max} x_{i,t} \qquad \left(\phi_{i,t}^{\hat{Q}^{max}}, \phi_{i,t}^{\hat{Q}^{min}}\right) \forall i \in \mathcal{I}_H, \forall t \in \mathcal{T} \tag{36}$$

$$Q_{r,t} = \sum_{i \in \mathcal{I}_H} q_{i,t} \qquad \left(\lambda_{r,t}^Q\right) \forall r \in \mathcal{R}, \forall t \in \mathcal{T} \Big\} \tag{37}$$

Expression (22) is the power balance, (23) to (26) model the DC approach, (27) to (30) model the thermal problem, including generation costs, ramp constraints and operating limits, while in (31) to (37) the hydro problem, which includes the linear production function, the water balance and its operational limits. It is noteworthy that the hydroelectric production function was linearized through a concave piecewise linear approximation, following [17].

Next to each constraint in the viability set $\Omega(x, v, u)$, the respective dual variables (λ and ϕ), are represented, as these will be considered to solve the problem. Thus, the complete mathematical formulation can be represented hierarchically according to (38) to (42).

$$z = \min_{x,v} \sum_{t=1}^{T} \sum_{i \in \mathcal{I}_K} \left(C_{i,t}^{SU} + C_{i,t}^{SD} + C_{i,t}^{NL} x_{i,t} \right) + \eta \qquad \textit{(Level 1)} \quad (38)$$

s.t:

Constraints (10) to (21) (39)

$$\eta = \max_{u \in \mathcal{U}} \delta \qquad \textit{(Level 2)} \quad (40)$$

s.t:

Constraints (2) to (8)

$$\delta = \min_{y \in \Omega(x,v,u)} \sum_{t=1}^{T} \sum_{i \in \mathcal{I}_K} C_{i,t}^{P} + \sum_{t=1}^{T} \sum_{r=1}^{\mathcal{R}} \hat{C}_{r,t}^{S} S_{r,t} \qquad \textit{(Level 3)} \quad (41)$$

s.t:

Constraints (22) to (37) (42)

Solution Methodology

The resulting model from the formulation consists on a three-level mixed integer linear optimization model. This kind of problem, three levels (two-stage), or even bi-level models (single stage), are known to be NP-hard, i.e., they are extremely difficult to solve [32], [33], [34], [35], [36]. Among the solutions used to solve this kind of problem is the column and constraint generation algorithm (C&CG). In general, this technique consists of decomposing the three-level model into two other problems: the main problem (master), which contains the first-stage decisions, and the subproblem, which contains the second-stage decisions. Unlike the Benders decomposition, the C&CG uses only information related to the primal decision variables to reconstruct the objective function of the main problem, which improves the convergence [10], [32].

Thus, the three-level model is solved using this approach where, in the main problem, the best UC decisions are defined and in the subproblem, the main problem decisions are fixed, and the best operational decisions given the worst realization of the uncertainties are identified. At the end of the subproblem resolution, the information related to the uncertainties is sent to the main problem, where they are fixed. At each iteration a new set of constraints is included to the main problem, where uncertainties are fixed according to each of the different scenarios visited – as represented in the flowchart of Figure 2.

The first level – main problem, is solved by approximating the function η through the set of primal constraints – (22) to (37). Thus, the main problem can be represented through the formulation (43) to (46).

$$\min_{x,v} \sum_{t=1}^{T} \sum_{i \in \mathcal{I}_K} \left(C_{i,t}^{SU} + C_{i,t}^{SD} + C_{i,t}^{NL} x_{i,t} \right) + \eta \quad (43)$$

s.t:

Constraints (10) to (21) (44)

Constraints (22) to (37) $\forall \omega' \leq \omega$ (45)

$$\eta \geq \sum_{t=1}^{T} \sum_{i \in \mathcal{I}_K} C_{i,t,\omega'}^{P} + \sum_{t=1}^{T} \sum_{r=1}^{\mathcal{R}} \hat{C}_{r,t}^{S} S_{r,t,\omega'} \qquad \forall \omega' \leq \omega \quad (46)$$

where ω' is the iteration counter of the problem, so $\omega' = 1, \ldots, \omega$, where ω is the total number of iterations (updated at each iteration). In this solution step, the optimization variables correspond to the commitment decisions of the units ($x_{i,t}, v_{i,t}^{SU}, v_{i,t}^{SD}$), the operating decisions ($C_{i,t,\omega'}^{P}, p_{i,t,\omega'}, P_{l,t,\omega'}, \theta_{n,t,\omega'}, q_{i,t,\omega'}, Q_{r,t,\omega'}, V_{r,t,\omega'}$, $S_{r,t,\omega'}$), and the auxiliary variable η, which is used to reconstruct the objective function gradually.

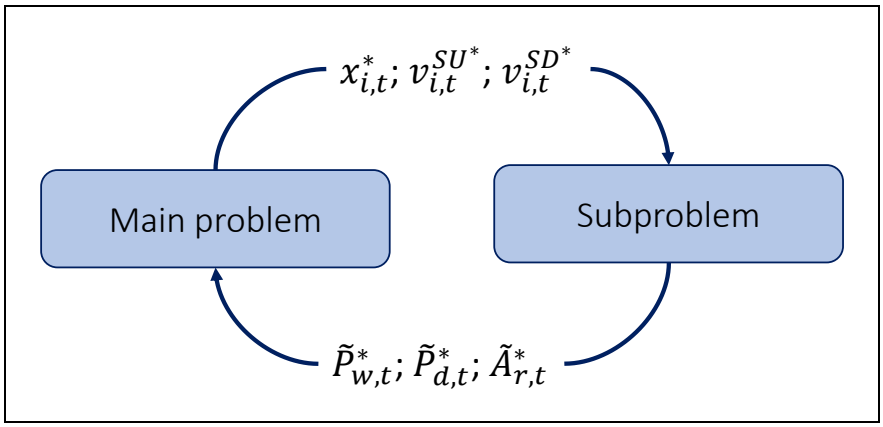

Figure 2. Solution framework for the two-stage robust optimization problem

The uncertainty parameters ($\tilde{P}_{w,t,\omega'}, \tilde{A}_{r,t\omega'}, \tilde{P}_{\mathrm{d},t\omega'}$), are fixed in their optimal values from the solution obtained in the subproblem for each of the iterations performed, being used as input into the main problem. The objective is to find a unique value for x and v, ensuring that the best operating point for the worst realization of uncertainty is being search. It is also noteworthy that the optimization variable η represents the objective function of the subproblem and there is a single η to be optimized in the main problem. Note that the main problem consists of a single-level MILP problem (minimization), since it includes binary decisions related to the UC problem, which can be solved through a conventional commercial solver.

Regarding to subproblem, it consists of the second and third level of solution as described between constraints (40) to (42). Because it is composed of two levels this cannot be solved directly as the main problem. Thus, the subproblem is solved through a single level equivalent model. As mentioned above, at each iteration a new set of commitment decisions is found in the main problem where, at each iteration, these optimal decisions related to binary variables are used as input data in the subproblem and are therefore fixed in the second stage of solution. Thus, a purely linear, continuous, and convex two-level model in its decision variables ($y \backslash (x, v) \in \Omega(x^*, v^*, u)$) is obtained in the subproblem, allowing it to be rewritten on a single equivalent level through the Karush-Kuhn-Tucker (KKT) conditions. Thus, the bilevel problem $\max_{u \in U} \min_{y} b^T y(u)$ is rewritten as $\max_{u \in U, y, \lambda, \phi} b^T y(u, \lambda, \phi)$ where y represents the optimization variables related to minimization subproblem; u represents the optimization variables related to maximization subproblem; λ is the dual variable related to equality constraints of the minimization subproblem; ϕ is the dual variable related to inequality constraints of the minimization subproblem. The resulting subproblem is a non-linear model due to complementarity constraints, which has the following format $0 \leq a \perp b \geq 0$. Such nomenclature is equivalent to the non-linear expression $a \geq 0$, $b \geq 0$ and $ab = 0$, which can be replaced by the equivalent mixed integer linear representation [32], also called the Big M method. Therefore, the final model obtained in the subproblem is a single level (maximization) mixed integer linear problem and can be solved using an available commercial solver. The steps followed to reformulate the subproblem (two level problem), using the KKTs were mainly based on [32], and the final formulation obtained is available in supplementary material for those who interested.

The two-stage solution procedure can be summarize as follow:

(1) An initial estimate is obtained to $\tilde{P}_{\mathrm{d},t}$, $\tilde{P}_{w,t}$ and $\tilde{A}_{r,t}$;
(2) Definition of upper and lower bounds: $UB = +\infty$ and $LB = -\infty$;
(3) The iteration counter is initialized ($\omega = 0$);
(4) Using the values obtained in (1), the main problem is solved, where the optimal values of $x_{i,t}^{*}$, $v_{i,t}^{SU*}$, $v_{i,t}^{SD*}$, η^{*}, $C_{i,t,\omega\prime}^{P*}$, $p_{i,t,\omega'}^{*}, P_{l,t,\omega'}^{*}$, $\theta_{n,t,\omega'}^{*}$, $q_{i,t,\omega'}^{*}$, $Q_{r,t,\omega'}^{*}$, $V_{r,t,\omega'}^{*}$, $S_{r,t,\omega'}^{*}$ are obtained;
(5) Update LB: $LB = \sum_{t=1}^{T} \sum_{i \in \mathcal{I}_K} \left(C_{i,t}^{SU} + C_{i,t}^{SD} + C_{i,t}^{NL} x_{i,t}^{*} + \eta^{*} \right)$;
(6) The subproblem is solved using information obtained in (4) as input data (fixed). The realization of uncertainties ($\tilde{P}_{w,t,\omega\prime}^{*}$, $\tilde{P}_{\mathrm{d},t,\omega\prime}^{*}$,$\tilde{A}_{r,t,\omega\prime}^{*}$) are then stored for later use as input to the main problem;

(7) Update UB: $UB = \min\{UB, \sum_{t=1}^{T}\sum_{i\in\mathcal{I}_K}\left(C_{i,t}^{SU} + C_{i,t}^{SD} + C_{i,t}^{NL}x_{i,t}^{*}\right) + \sum_{t=1}^{T}\sum_{i\in\mathcal{I}_K} C_{i,t}^{P*} + \sum_{t=1}^{T}\sum_{r=1}^{\mathcal{R}} \hat{C}_{r,t}^{S}S_{r,t}^{*}\}$;
(8) The convergence between stages is checked as a relative error between the two solution stages (tol);
(9) If convergence does not occur, the iteration counter is updated and the process continues to occur from (4), using the information found in (6), until the convergence value is within the tol.

RESULTS AND DISCUSSIONS

Test systems

The Python 3.8 language and the Gurobi 9.0.2 solver was used to solve the models. A laptop with an Intel® Core™ i5-3230M CPU @ 2.60GHz, with 4.00 GB RAM was used to carry out the simulations.

Two test systems were considered to perform the simulations and validate the proposed model: (1) 30 buses IEEE test system (30-IEEE) adapted from [17] and [37]; (2) 33 buses southern Brazilian test subsystem from the national interconnected system (33-BTS), adapted from [38] and [39]. In both test systems hydroelectric generation capacity is predominant in the system. Also, in both cases, the total demand is expressed as a percentage of the system's total generation capacity, with the maximum demand occurring at 6 p.m. To thermoelectric and hydroelectric plants, it was considered that each plant is composed of only one generating unit, given the similar characteristic, which is a common practice in the literature, such is done in [16] and [17].

The hydroelectric production function is represented by a piecewise linear approximation function, which is concave to ensure the model's convexity [17]. In the 30-IEEE test system, this linearization was used according to [17]. In the 33-BTS, only a linear segment was considered, which would be equivalent to the model with constant productivity, a practice also found in the literature, as for example in [40], [41], [42], [43] and [44]. Other iterative processes, or methodologies could be used to perform this linearization, however details like that are not within the scope of this study. The complete data and other information regarding the test systems used can be verified in the supplementary material.

Given these test systems, different scenarios were verified using different values for Γ. The scenarios presented in Table 1 and Table 2 were considered of greater relevance to discuss. The ones highlighted, called “main scenarios”, will be discussed more closely. Regarding the analyzed uncertainty levels, a Γ between 0 and 0.20 and 0.25 was considered, however, Γ can have any value between 0 and 1. The choice of Γ studied in this work was carried out regarding variations closer to what could occur in a real situation.

Table 1. 30-IEEE Operation Costs Results and Simulation Times

Γ^W, Γ^H	Γ^D				
	0.00	**0.10**	**0.15**	**0.20**	**0.25**
0.00	$55	$106.94	$1069.93	$2 857.58	$5 521.41
	364.57s	59.99s	591.6s	5478.91s	14706s
0.10	$55	$222.62	$1180.61	$3169.89	$5 833.72
	63.42s	64.15s	355s	4361.19s	697.41s
0.15	$55.00	$277.96	$1 240.95	$3 326.05	$6 000.88
	36.96s	33.49s	458.27s	5649.5s	606.86s
0.20	$55.00	$333.30	$1 296.29	$3 482.21	$6 287.51
	46.76s	32.64s	2388.11s	1949.33s	230.35s
0.25	$55.00	$388.64	$1 351.63	$3638.36	$6 489.15
	29.75s	41.37s	3900.73s	3177.74s	145.67s

Table 2. 33-BTS Operation Costs Results and Simulation Times

Γ^W, Γ^H	Γ^D			
	0.00	**0.10**	**0.15**	**0.20**
0.00	$0.00	$11500.00	$26696.61	$30282.21
	38.53s	27.97s	72.28s	57.36s
0.10	$0.00	$11500.00	$26718.21	$30466.54
	15.01s	52.22s	97.13s	104.54s
0.15	$11500.00	$11518.96	$26820.12	$30615.93
	16.9s	27.89s	1650.61s	47.91s
0.20	$11500.00	$23399.77	$27059.82	$30797.39
	16.28s	32.19s	289.25s	144.92s

Considerations to computer simulations

To perform the computer simulations, some improvements were made to the proposed mathematical model: (1) The normalization of operating costs, i.e., the objective function was divided by 1000, for both test systems. This strategy does not affect the final solution of the problem, it only improves the convergence times of the simulated models; (2) Expressions (2), (4), (6) and (7) were rewritten by replacing the inequality sign with the equality sign in order to reduce the solution search space. This is possible because the optimal solution of the proposed model is always found at the extremes of the sets of polyhedral uncertainties [20]; (3) A penalty for spillage was considered – Expression (9), in order to avoid the occurrence of unwanted spillages. As discussed, the spillage decision, as well as its fictitious cost, is a second stage decision. However, it was found that the addition of the spill cost in the subproblem makes this solution computationally intractable. Thus, in order to improve the convergence time and continue using this spill cost to obtain an improved solution, a small spill cost was added to the main problem – constraint (46). This was assumed as $1x10^{-3}$ and $1x10^{-1}$ for 30-IEEE and 33-BTS, respectively. Note that this change is only possible because the occurrence of unnecessary spillages in the original model does not impact the generation decision cost, and therefore has no impact on the problem final solution; (4) The variable M, from Big M method that was used to linearize the complementarity constraints resulting from the KKTs, was defined as the lowest possible value that does not change the final result. These definitions were made following what is suggested in [45], since the definition of a good value of M is very important to guarantee the computational tractability of the model. The final values of M used in the present work, as well the other specifications, can be checked in the supplementary material for those interested.

Results analysis

The results related to the total operating costs ($) and the time (in seconds) of simulations obtained for test systems are presented in Table 1 and Table 2. It is observed, that there is an increase concerning the total operating cost as Γ increases. For example, in 30-IEEE, there is an increase of about $6106.53 in operating costs related to thermal generation from scenario where $\Gamma^{\mathcal{D}} = \Gamma^{W} = \Gamma^{H} = 0.10$ to scenario where $\Gamma^{\mathcal{D}} = \Gamma^{W} = \Gamma^{H} = 0.25$, in order to meet the systems requirements, as represent in Figure 3.

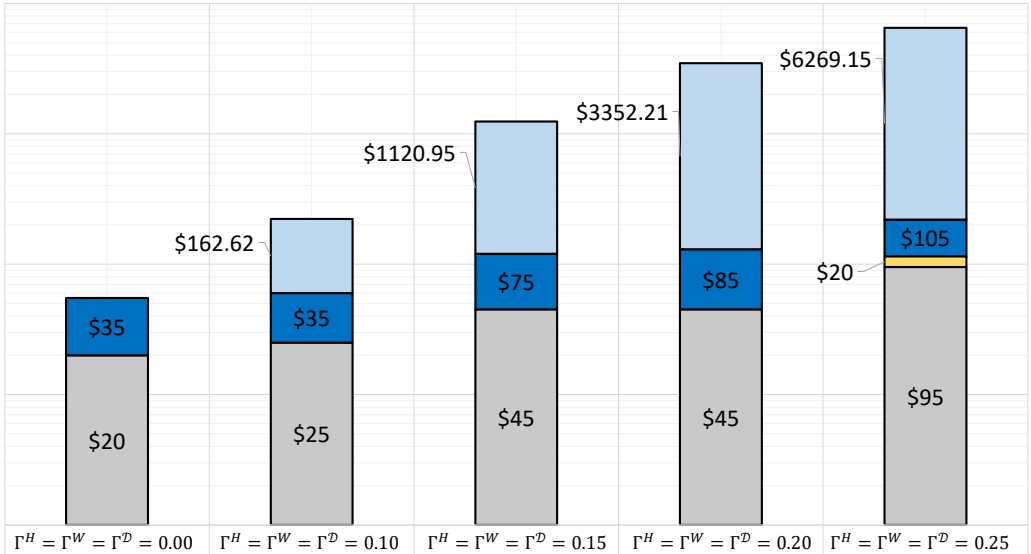

	$\Gamma^{H} = \Gamma^{W} = \Gamma^{\mathcal{D}} = 0.00$	$\Gamma^{H} = \Gamma^{W} = \Gamma^{\mathcal{D}} = 0.10$	$\Gamma^{H} = \Gamma^{W} = \Gamma^{\mathcal{D}} = 0.15$	$\Gamma^{H} = \Gamma^{W} = \Gamma^{\mathcal{D}} = 0.20$	$\Gamma^{H} = \Gamma^{W} = \Gamma^{\mathcal{D}} = 0.25$
Thermal generation	0.00%	73.05%	90.33%	96.27%	96.61%
Status on	63.64%	15.72%	6.04%	2.44%	1.62%
Shutdown	0.00%	0.00%	0.00%	0.00%	0.31%
Start up	36.36%	11.23%	3.63%	1.29%	1.46%

Figure 3. Operating total costs for the 30-IEEE in the main scenarios. The logarithmic scale is used to demonstrate more clearly the results obtained graphically. In addition to the operating costs ($) shown in the graph, a table with the percentage that each cost represents of the total amount of operation is also added below.

Likewise, there is an increase in costs related to the start up decisions, since the energy reserve requirements also starts to increase due to the variability in demand, resulting from Γ. Also, the thermal units need to be on for longer periods, or more plants need to be start up and consequently kept on, as higher is the assumed Γ – for $\Gamma^{\mathcal{D}} = \Gamma^{W} = \Gamma^{H} = 0$, for example, the start up cost is \$35.00 and for 0.25 this cost becomes \$105.00. In both test systems, even the hydro units having enough energy to meet the demand, it was necessary to turn on the thermal plants, since the water volume targets for the last period of operation must be met. Likewise, it is often necessary to keep the thermal units on, in order to comply with the minimum start up and shutdown times, as well as ramp constraints.

Regarding the simulation time, there was no pattern that relates the computational time with the assumed Γ, however it is worth mention the improvements resulting from the computational adjustments carried out, like the adjustment of the sign in the uncertainty sets, described in the subsection *Considerations to computer simulations*. For 30-IEEE, for example, in scenario where $\Gamma^{\mathcal{D}} = \Gamma^{W} = \Gamma^{H} = 0.20$ without using the equal sign, the total simulation time was 11405 seconds, just over 3 hours of simulation, while using the signal of equality a computational time of 1949 seconds, just over 32 minutes, was obtained. The same objective function value was found in both simulated scenarios, but with a difference of more than two and a half hours between the times of the two simulations performed.

Regarding the uncertainty variation impact on UC decisions, it was found, that the activation of the hydro units are prioritized, and the thermal units are activated only in specific periods to meet demand or reserve requirements. In the 30-IEEE, for example, even with $\Gamma^{\mathcal{D}} = \Gamma^{W} = \Gamma^{H} = 0$, there is a need to turn on at least one thermal unit to meet the requirements. As Γ increases, it is necessary to turn on a greater number of units, or even units with greater generation capacity, capable of meeting the variability resulting from the adopted Γ. In the 33-BTS, a similar behavior is verified. Due to the characteristics of the system, with great wind participation and a large hydro generation available, the activation of the thermal units starts to occur from $\Gamma^{\mathcal{D}} = \Gamma^{W} = \Gamma^{H} = 0.10$. In this scenario starts up only 1 thermal machine is enough to meet demand and reserve requirements, while in the other main scenarios both available units are necessary. The generation of thermal energy to meet the demand grows from 215MW in scenario where $\Gamma^{\mathcal{D}} = \Gamma^{W} = \Gamma^{H} = 0.15$, to 443MW in scenario where $\Gamma^{\mathcal{D}} = \Gamma^{W} = \Gamma^{H} = 0.20$.

Regarding the water balance, in the 30-IEEE system, the results obtained were consistent. It was found that the addition of the spillage cost, was very positive for the system. In the scenario where $\Gamma^{\mathcal{D}} = \Gamma^{W} = \Gamma^{H} = 0.15$, for example, there was a decrease from 295.39hm³ to 0hm³ in the occurrence of unwanted spillages. Meanwhile in scenario where $\Gamma^{\mathcal{D}} = \Gamma^{W} = \Gamma^{H} = 0.20$, for 33-BTS, the spillage applying to the costs had a reduction of more than 465hm³. In both test systems the same final result was obtained with and without the costs applied.

Finally, regarding the constraints related to transmission network system, it is worth mentioning the behavior of 33-BTS test system, where some transmission lines, most of them directly connected to demands, reached their limits in the different simulated scenarios. So varying Γ it is possible to notice which lines reach their limits, and such information can be useful for the energy system operator in order to study and avoid possible system bottlenecks, ensuring reliable operating conditions.

Discussions regarding the computational costs

The optimization problem presented showed great challenges in computational terms. Without the adjustments described in the subsection *Considerations to computer simulations*, many simulated scenarios had prohibitive simulation times (more than 24 hours) and in some cases they even caused memory errors, preventing the iterations from being completed. Therefore, the presentation of some findings in this work can contribute to possible future studies.

In order to identify the causes of this computational costs, a study of the constraints in the different stages of the model solution was carried out. It was found that although the main problem grows as the number of iterations also grows, the longer computational times are related to the subproblem, that is, the second stage decisions. The subproblem, as discussed, has a very complex combinatorial nature due to the methodology used to linearize the complementarity constraints – the Big M method together with binary variables. So, this linearization methodology may be one of the bottlenecks in the solution optimization process of the second stage, which is also pointed out in some studies such as [6] and [13]. Another point are the constraints with temporal (ramp constraints and water balance) and spatial (cascading plants) coupling and their respective expressions related to KKTs, where the intertemporal and spatial nature is naturally extended. Thus, the improvements proposed in the subsection *Considerations to computer simulations* are very important contributions of this work, since such adjustments allowed an improvement in computational costs.

CONCLUSION

In the present work, a computational model was proposed applying robust optimization to the day-ahead UC problem of a hydro-thermal-wind power system. Uncertainties in demand, wind power and water inflow were considered, as well as a DC model of the transmission network and energy reserve requirements. The final model was computationally implemented using the Python 3.8 programming language.

One of the main contributions of the present work involves the uncertainties water inflow modeling considering the spatial and temporal water problem relation through a polyhedral uncertainty set. In addition, it is considered in a problem that also deals with uncertainties in demand and wind generation. The use of the piecewise linear approximation to the hydroelectric production function is also considered of great relevance, since it allows the incorporation of important characteristics of the water problem to the optimization under uncertainties.

The proposed optimization model also allowed the application of the C&CG algorithm for its resolution, which is commonly used in the literature. The complete model and its solution allowed identifying important aspects related to the computational costs, verifying that the constraints that couple the problem in space and time have a significant influence on the simulation times, as well as the combinatory nature of the subproblem, due to the use of the Big M methodology to linearize the complementarity constraints.

Some strategies in order to reduce computational costs were adopted, such as adjusting the value of M and changing the sign of the uncertainty sets, which allowed the achievement of scenarios with consistent results in reasonable simulation times given the dimensions of the test systems considered.

Through the computer simulations carried out, it was also verified that the system is capable of prioritizing the most economical energy sources. As the level of uncertainty in generation, water inflow and demand increases, a greater use of thermal plants is required, either to meet demand, or to meet reserve requirements. In one of the simulated scenarios, it was also possible to verify that the increase in the uncertainty budget, also impacts the power flow through the transmission lines, causing the operational limits to be reached for longer periods of time, and for more transmission lines, as the level of uncertainty also grows. The study of this behavior can be very useful for the electrical power system operator in the sense that the variations in uncertainty levels can demonstrate possible bottlenecks in the system, such as the need to increase the transmission limits of certain points in the system.

An important observation is that higher levels of uncertainty can be simulated through the proposed model, higher than the maximum uncertainty level of 0.25 adopted in the present study. However, it may happen that in certain cases the models do not identify a feasible solution, indicating the need for some action related to the expansion of the system, so that it can support possible variability of the uncertainties considered. One way to carry out this study is to incorporate load shedding into the problem, which is a suggestion for future work.

Furthermore, it is worth noting that due to the nature of two-stage decision making, the essential solution for the robust model proposed in the present study is first-stage decisions, while second-stage decisions are made with perfect information about uncertainties. This is the case of many of the works mentioned throughout the literature review of this study, and a way to circumvent this limitation is to use multistage optimization models that employ the so-called decision rules, which is also a guideline for the development of future works, aimed at optimization under uncertainty.

Finally, it is concluded that the robustness of the solution in the proposed model, can be controlled through the level of uncertainty. The higher the level of uncertainty considered, the worse the simulated operating conditions are, and consequently the higher the associated operating costs. This allows the operator of the electric power system to prepare for the occurrence of unexpected situations in the operation planning, and take preventive actions to guarantee the safe and reliable system operation. Thus, robust optimization can be seen as a preventive view of what can happen during the operation of the electric power system, being used by the central operator as a basis to taking important decisions in real-time operation and in the improvement on the operation planning and expansion of the electric power systems.

Funding: This study was financed in part by the CAPES, Brazil.
Conflicts of Interest: The authors declare no conflict of interest.
Supplementary Material: This article has supplementary material. Available in:
https://www.documentador.pr.gov.br/documentador/pub.do?action=d&uuid=@gtf-escriba-tecpar@b5838833-735c-48ae-b56e-45bd3e766ff1

REFERENCES

1. Lorca A, Sun XA. Adaptive Robust Optimization with Dynamic Uncertainty Sets for Multi-Period Economic Dispatch Under Significant Wind. IEEE Trans Power Syst. 2015 Jul; 30(4):1702–13.
2. Jiang R, Zhang M, Li G, Guan Y. Two-Stage Robust Power Grid Optimization Problem. J. Oper. Res. 2010; 1–34.
3. Quan H, Srinivasan D, Khambadkone AM, Khosravi A. A Computational Framework for Uncertainty Integration in Stochastic Unit Commitment with Intermittent Renewable Energy Sources. Appl Energy. 2015 Aug; 152:71–82.
4. Alem D, Morabito R. [Production Planning Under Uncertainty: Stochastic Scheduling Versus Robust Optimization]. Gest Prod. 2015 Sep 29; 22(3):539–51.
5. Street A, Oliveira F, Arroyo JM. Contingency-Constrained Unit Commitment with Security Criterion: A Robust Optimization Approach. IEEE Trans Power Syst. 2011 Aug; 26(3):1581–90.
6. Wang Q, Watson J, Guan Y. Two-Stage Robust Optimization for N-K Contingency-Constrained Unit Commitment. IEEE Trans Power Syst. 2013 Aug; 28(3):2366–75.
7. Street A, Moreira A, Arroyo JM. Energy and Reserve Scheduling Under a Joint Generation and Transmission Security Criterion: An Adjustable Robust Optimization Approach. IEEE Trans Power Syst. 2014 Jan; 29(1):3–14.
8. Moreira A, Street A, Arroyo JM. An Adjustable Robust Optimization Approach for Contingency Constrained Transmission Expansion Planning. IEEE Trans Power Syst. 2015 Jul; 30(4):2013–22.
9. Moreira A, Street A, Arroyo JM. Energy and Reserve Scheduling Under Correlated Nodal Demand Uncertainty: An Adjustable Robust Optimization Approach. Int J. Electr. Power Energy Syst. 2015 Nov; 72:91–8.
10. Long Zhao, Bo Zeng. Robust Unit Commitment Problem with Demand Response and Wind Energy. In: 2012 IEEE Power and Energy Society General Meeting. San Diego, CA: IEEE; 2012. p. 1–8. Available from: http://ieeexplore.ieee.org/document/6344860/
11. Bertsimas D, Litvinov E, Sun XA, Zhao J, Zheng T. Adaptive Robust Optimization for the Security Constrained Unit Commitment Problem. IEEE Trans Power Syst. 2013 Feb; 28(1):52–63.
12. Jiang R, Zhang M, Li G, Guan Y. Two-Stage Network Constrained Robust Unit Commitment Problem. Eur J Oper Res. 2014 May; 234(3):751–62.
13. An Y, Zeng B. Exploring the Modeling Capacity of Two-Stage Robust Optimization: Variants of Robust Unit Commitment Model. IEEE Trans Power Syst. 2015 Jan; 30(1):109–22.
14. Lorca A, Sun XA, Litvinov E, Zheng T. Multistage Adaptive Robust Optimization for the Unit Commitment Problem. Oper. Res. 2016 Feb; 64(1):32–51.
15. Amjady N, Dehghan S, Attarha A, Conejo AJ. Adaptive Robust Network-Constrained AC Unit Commitment. IEEE Trans Power Syst. 2017 Jan; 32(1):672–83.
16. Jiang R, Wang J, Guan Y. Robust Unit Commitment with Wind Power and Pumped Storage Hydro. IEEE Trans Power Syst. 2012 May; 27(2):800–10.
17. Dashti H, Conejo AJ, Jiang R, Wang J. Weekly Two-Stage Robust Generation Scheduling for Hydrothermal Power Systems. IEEE Trans Power Syst. 2016 Nov; 31(6):4554–64.
18. Wu W, Chen J, Zhang B, Sun H. A Robust Wind Power Optimization Method for Look-Ahead Power Dispatch. IEEE Trans Sustain Energy. 2014 Apr; 5(2):507–15.
19. Zugno M, Conejo AJ. A Robust Optimization Approach to Energy and Reserve Dispatch in Electricity Markets. Eur J Oper Res. 2015 Dec; 247(2):659–71.
20. Attarha A, Amjady N, Conejo AJ. Adaptive Robust Ac Optimal Power Flow Considering Load and Wind Power Uncertainties. Int J. Electr. Power Energy Syst. 2018 Mar; 96:132–42.
21. Reddy SS. Optimal Scheduling of Thermal-Wind-Solar Power System with Storage. Renew Energy. 2017 Feb; 101:1357–68.
22. Reddy SS. Optimal Scheduling of Wind-Thermal Power System Using Clustered Adaptive Teaching Learning Based Optimization. Electr Eng. 2017 Jun; 99(2):535–50.
23. Reddy SS. Optimal Power Flow Using Multi-Objective Glowworm Swarm Optimization Algorithm in A Wind Energy Integrated Power System. Int. J. Green Energy. 2019 Dec 8; 16(15):1547–61.
24. Reddy SS. Multi-Objective Optimal Power Flow for a Thermal-Wind-Solar Power System. JGE. 2018; 7(4):451–76.
25. Reddy SS, Momoh JA. Minimum Emissions Optimal Power Flow in Wind-Thermal Power System Using Opposition Based Bacterial Dynamics Algorithm. In: 2016 IEEE Power and Energy Society General Meeting (PESGM). Boston, MA, USA: IEEE; 2016. p. 1–5. Available from: http://ieeexplore.ieee.org/document/7741635/
26. Reddy SS, Sandeep V, Chitti B, Jung CM. Multi-Objective Based Optimal Generation Scheduling Considering Wind and Solar Energy Systems. Int. J. Emerg. Electr. Power Syst. 2018 Oct 25; 19(5). Available from: https://www.degruyter.com/document/doi/10.1515/ijeeps-2018-0006/html
27. Reddy SS. Multi-Objective Based Economic Environmental Dispatch with Stochastic Solar-Wind-Thermal Power System. IJECE. 2020 Oct 1; 10(5):4543-51.
28. Ben-Tal A, El Ghaoui L, Nemirovskij A. Robust optimization. Princeton: Princeton University Press; 2009. (Princeton series in applied mathematics).
29. Hedman KW, Korad AS, Zhang M, Thompson G, Dominguez-Garcia A, Jiang X. The Application of Robust Optimization in Power Systems. Power Systems Engineering Research Center: Arizona State University; 2014 p. 174. Report No.: PSERC Publication: 14-6. Available from: https://pserc.wisc.edu/wp-content/uploads/sites/755/2018/08/S-51_Final-Report_Sept-2014.pdf

30. Dunning IR. Advances in Robust and Adaptive Optimization: Algorithms, Software, and Insights [PhD Thesis]. Massachusetts Institute of Technology; 2016.
31. Nazari-Heris M, Mohammadi-Ivatloo B. Application of Robust Optimization Method to Power System Problems. In: Classical and Recent Aspects of Power System Optimization. Elsevier; 2018. p. 19–32. Available from: https://linkinghub.elsevier.com/retrieve/pii/B9780128124413000021
32. Conejo AJ, Baringo L, Kazempour SJ, Siddiqui AS. Investment in Electricity Generation and Transmission. Cham: Springer International Publishing; 2016. Available from: http://link.springer.com/10.1007/978-3-319-29501-5
33. Hansen P, Jaumard B, Savard G. New Branch-and-Bound Rules for Linear Bilevel Programming. SIAM J Sci Stat Comput. 1992 Sep; 13(5):1194–217.
34. Zeng B, Zhao L. Solving Two-Stage Robust Optimization Problems Using A Column-and-Constraint Generation Method. Oper. Res. Lett. 2013 Sep; 41(5):457–61.
35. Hart WE, Watson J, Siirola JD, Chen R. Modeling Bilevel Programs in Pyomo. Sandia National Lab. (SNL-NM), Albuquerque, NM (United States); Sandia; 2016.
36. Sinha A, Malo P, Deb K. A Review on Bilevel Optimization: From Classical to Evolutionary Approaches and Applications. IEEE Trans Evol Computat. 2018 Apr; 22(2):276–95.
37. Zimmerman RD, Murillo-Sanchez CE, Thomas RJ. MATPOWER: Steady-State Operations, Planning, and Analysis Tools for Power Systems Research and Education. IEEE Trans Power Syst. 2011 Feb; 26(1):12–9.
38. Alves W. [Proposition of Test Systems for Power Systems Computational Analysis] [PhD Thesis]. Niterói: Universidade Federal Fluminense; 2007. 332p. Available from: https://www.sistemas-teste.com.br/arquivos/Dissertacao.pdf
39. Fabrício Yutaka Kuwabata Takigawa. [Development of A Computational Model for The Hydrothermal Systems Daily Operation Scheduling]. [PhD Dissertation]. Florianópolis: Universidade Federal de Santa Catarina; 2010. 212p. Available from: https://repositorio.ufsc.br/xmlui/bitstream/handle/123456789/94379/286903.pdf?sequence=1&isAllowed=y
40. Alguacil N, Conejo AJ. Multiperiod Optimal Power Flow Using Benders Decomposition. IEEE Trans Power Syst. 2000 Feb; 15(1):196–201.
41. Simopoulos DN, Kavatza SD, Vournas CD. An Enhanced Peak Shaving Method for Short Term Hydrothermal Scheduling. Energy Convers. Manag. 2007 Nov; 48(11):3018–24.
42. Sifuentes W, Vargas A. Short-Term Hydrothermal Coordination Considering an Ac Network Modeling. International Int J. Electr. Power Energy Syst. 2007 Jul; 29(6):488–96.
43. Sifuentes W, Vargas A. Short-Term Hydrothermal Optimization with Congestion and Quality of Service Constraints. IET Gener Transm Distrib. 2007; 1(4):574.
44. Frangioni A, Gentile C, Lacalandra F. Tighter Approximated MILP formulations for Unit Commitment Problems. IEEE Trans Power Syst. 2009 Feb; 24(1):105–13.
45. Gabrel V, Lacroix M, Murat C, Remli N. Robust Location Transportation Problems Under Uncertain Demands. Discrete Applied Mathematics. 2014 Feb; 164:100–11.